Writing F_∞ for the two-dimensional map corresponding to $\beta = +\infty$, simple computations (see the proof of Lemma 1 in the Appendix) show that the first two iterates of the unstable segment EA_0 are (see Figures 6a–b)[13]

(3.13a) $F_\infty(EA_0) = EA_1$,

(3.13b) $F_\infty^2(EA_0) = F_\infty(EA_1) = EA_1^* \cup B_0 A_2$.

The third and fourth iterates of the segment EA_0 depend upon the market instability ratio b/B. For $1 < b/B < (1+\sqrt{5})/2$ we get (Figure 6a)

(3.14a) $F_\infty^3(EA_0) = F_\infty(EA_1^* \cup B_0 A_2) = EA_1 \cup B_0^* A_2^* \cup A_2^* C_1^+ \cup A_0^* E$,

(3.14b) $F_\infty^4(EA_0) = EA_1^* \cup B_0 A_2 \cup A_2 C_1^{+*} \cup A_0 E \cup EA_1^* \cup A_1^* E$,

whereas for $b/B > (1+\sqrt{5})/2$ (Figure 6b)

(3.15a) $F_\infty^3(EA_0) = F_\infty(EA_1^* \cup B_0 A_2) = EA_1 \cup B_0^* A_2^* \cup A_2^* C_1^+ \cup A_0^* E \cup G$,

(3.15b) $F_\infty^4(EA_0) = EA_1^* \cup B_0 A_2 \cup A_2 C_1^{+*} \cup A_0 E \cup G \cup EA_1^* \cup A_1^* E$.

Notice that in these unions some segments have been included more than once, to emphasize the dynamics of F_∞^j, $1 \le j \le 4$, as a point X moves from E to A_0. Similarly, iterates $F_\infty^j(EA_0^*)$, $1 \le j \le 4$, of the symmetric opposite unstable segment EA_0^* are obtained.

A Large, But Finite Intensity of Choice β

The limiting case $\beta = +\infty$, where in each period all agents choose the optimal predictor, is important in understanding the case with a large but finite intensity of choice. In particular, the first four iterations of the unstable segment EA_0, for $\beta = +\infty$, yield important insight into the geometric shape of the unstable manifold of the steady state for $\beta < +\infty$, but large. There are in fact two possible cases for the global configuration of the unstable manifold, depending upon the market instability ratio b/B.

LEMMA 1 ("Almost Homoclinic Tangency Lemma"): *Let $C > 0$ and $b/B > 1$. For any $\varepsilon > 0$, there exists a β_c such that for all $\beta > \beta_c$, the unstable manifold $W^u(E)$ satisfies:*

(i) *if $1 < b/B < (1+\sqrt{5})/2$, then the first part of the right (left) branch of $W^u(E)$ is ε-close to the piecewise linear segment $EA_1^* B_0 A_2 C_1^{+*} A_0 EA_1^* E$ ($EA_1 B_0^* A_2^* C_1^+ A_0^* EA_1 E$) (Figure 6a);*

(ii) *if $b/B > (1+\sqrt{5})/2$, then the first part of the right (left) branch of $W^u(E)$ is ε-close to the piecewise linear segment $EA_1^* B_0 A_2 C_1^{+*} A_0 EGEA_1^* E$ ($EA_1 B_0^* A_2^* C_1^+ A_0^* EGEA_1 E$) (Figure 6b).*

[13] The following points are used: $A_j = F_\infty^j(A_0)$, $j = 1, 2$; $B_0 = ((b/B)C', +1)$; $C_1^+ = (-C', +1)$; and $G = (0, +1)$ (cf. the proof of Lemma 1). Moreover, X^* denotes the reflection point of X with respect to the m-axis. In the construction below, vertical segments joining the discontinuity points are included (cf. the proof of Lemma 1).

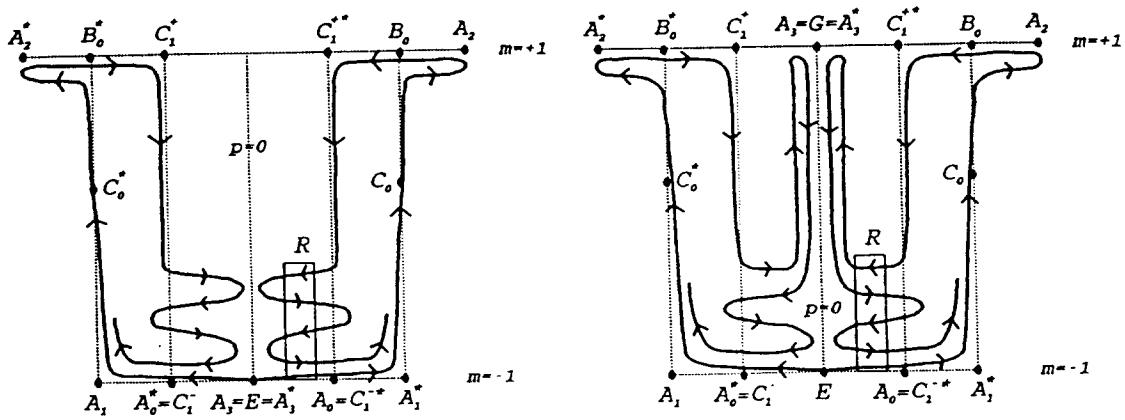

(a)-(b) The two different cases for the unstable manifolds of F_β for β large, with (a) $1 < b/B \leq (1 + \sqrt{5})/2$ and (b) $b/B > (1 + \sqrt{5})/2$.

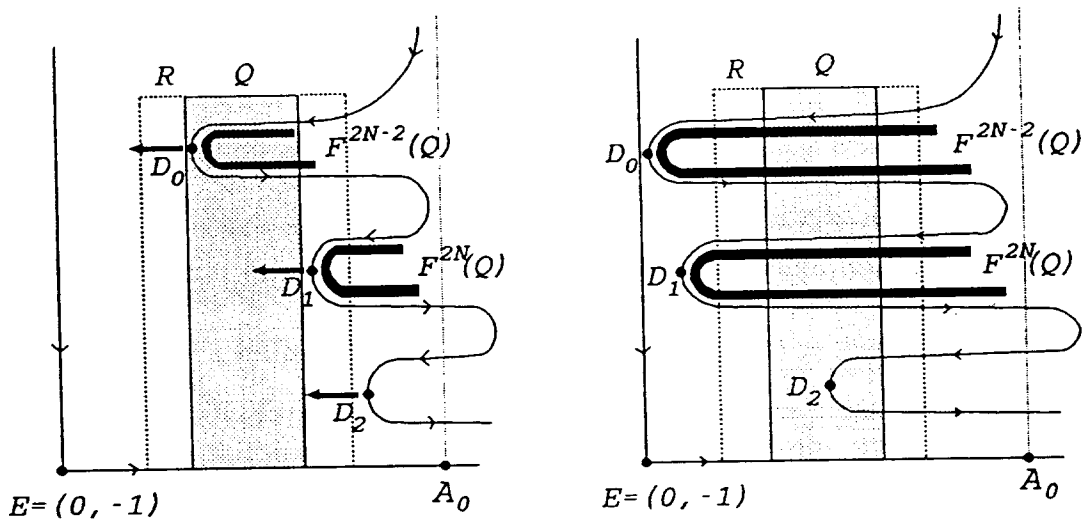

(c)-(d) Creation of horseshoes for the $2N$th iterate F^{2N}, as β increases.

FIGURE 6.

Both the formulation and the proof of this lemma are geometric rather than analytic, as is often the case in nonlinear dynamics. We emphasize though that this is a formal lemma, which is not based upon (but very much inspired by) computer simulations. According to the lemma, in both cases, for high values of the intensity of choice β the unstable manifold first moves away from the steady state when most agents use naive expectations, but later on returns close to the steady state when most agents switch to rational expectations. Hence, when the intensity of choice to switch predictors is large, the system is close to having a homoclinic orbit.

The reader should now compare the numerically obtained Figure 5 or the "theoretical" Figure 6 of the unstable manifold of the steady state, to the homoclinic bifurcation in Figure 4. There is an important difference. In our model, as β increases, a homoclinic bifurcation between the stable and unstable manifolds of the steady state does *not* occur. Although they get arbitrarily close, there can be no homoclinic intersection between the stable and unstable

manifolds of the *steady state*. This follows by noting that, for $m < +1$, deviations from the steady state price always change sign in the next period. Consequently, the unstable manifold of the steady state can never intersect the line-segment $p = 0$ in the stable manifold. Therefore, we refer to Lemma 1 as the "almost homoclinic tangency" or the "homoclinic kissing lemma." The lemma does not imply the occurrence of chaotic equilibrium time paths yet. However, using the geometric shape of the unstable manifold $W_\beta^u(E)$, we will show that, as β increases, there must be homoclinic bifurcations associated to dissipative *periodic saddle points*. In order to do so, we first show the following lemma.

LEMMA 2 ("Horseshoe Lemma"): *Assume $C > 0$ and $b/B > 1$. There exists a parameter value $\hat{\beta}$, such that for all $\beta > \hat{\beta}$ the fourth iterate F_β^4 has a horseshoe. Hence, for all $\beta > \hat{\beta}$ the A.R.E.D. is topologically chaotic.*

In Figure 6a–b we have indicated a rectangular region R which is mapped over itself in the form of a horseshoe by the fourth iterate F_β^4. Figures 6c and 6d illustrate the creation of a horseshoe for the map F_β^{2N}, $N \geq 2$, as the intensity of choice β increases. With increasing β, the image $F_\beta^{2N}(Q)$, lying close to the unstable manifold of the steady state, is folded and stretched, moving towards the stable manifold $W_\beta^s(E)$, over the rectangular subregion Q. The way in which these horseshoes are created implies that there must be homoclinic bifurcations associated to period $2N$ saddles:

LEMMA 3 ("Period $2N$ Homoclinic Bifurcation Lemma"): *For $N \geq 2$ sufficiently large, as β increases from 0 to $+\infty$, there exists a parameter value β_h, for which a homoclinic bifurcation between the stable and unstable manifolds of a dissipative (i.e. with corresponding eigenvalues λ and μ of JF^{2N} with $|\lambda\mu| < 1$) period $2N$ saddle point occurs.*

Applying the "strange attractor theorem" as discussed in Subsection 3.3, we get existence of strange attractors for a large set of parameters:[14]

THEOREM 3.3: *For generic demand and supply curves, C^2-close to the linear curves, in the cobweb model with rational versus naive expectations strange attractors exist for a positive Lebesgue measure set of (large) β-values.*

Notice that the period $2N$ saddles and the homoclinic bifurcations of Lemma 3 occur close to the unstable manifold of the steady state. In fact, in the first $2N - 2$ periods of the period $2N$ orbit almost all agents are naive and prices slowly diverge away from the steady state, whereas in the last two periods almost

[14] The theorem holds for demand and supply curves close to the linear ones, whenever the generic conditions concerning homoclinic bifurcations, or Takens' weaker conditions (see footnote 10) hold. In particular, in the special case of linear demand and supply, Takens' conditions are satisfied.

all agents become rational and prices return close to the steady state. Equilibrium time paths converging to the strange attractors in Theorem 3.3 are therefore characterized by an irregular switching between a phase where most agents are naive with prices close to the steady state and slowly diverging, and a phase where most agents are rational and prices are pushed back close to the steady state.

There is a close connection between the creation of homoclinic orbits, its associated strange attractors and the underlying *economic mechanism*. In stable phases with prices close to the steady state, "free riding" occurs and most agents switch to the cheap predictor. As a result an unstable phase with fluctuating prices sets in. In order to optimize their net profits in the unstable phase, agents are willing to pay the information costs and obtain the rational expectations forecast. When the intensity of choice is high, most agents switch to rational expectations, causing prices to return close to their steady state and the story repeats. The result is a "near" homoclinic tangency and an irregular switching between cheap "free riding" and expensive sophisticated prediction. One might summarize the complicated equilibrium dynamics as: "*high rationality in an unstable market with information costs implies chaos.*"

3.5. *Coexistence of Attractors*

For large values of the intensity of choice, the A.R.E.D. can be complicated and strange attractors can occur. For intermediate β-values there is another source of complicated dynamics, however, which has received relatively little attention in the economic literature, namely *coexistence of* (low periodic) *attractors*. In the presence of (small) noise coexisting attractors can be an important source of complicated dynamical behavior, since, as we will see, orbits may jump from one basin of attraction to the other in an irregular way.

Recall from Subsection 3.2 that, when β increases, the primary bifurcation is a period doubling from a stable steady state to a (symmetric) stable two-cycle. In the secondary bifurcation, the two-cycle loses stability and two coexisting stable four-cycles are created (Figure 1a–b).[15] We have the following theorem:

THEOREM 3.4 (Secondary Bifurcation): *Let β_1 be the primary bifurcation value in which the two-cycle $\{(\tilde{p},\tilde{m}),(-\tilde{p},\tilde{m})\}$ is created. There exists $\beta_2 > \beta_1$ such that:*

(i) *the two-cycle $\{(\tilde{p},\tilde{m}),(-\tilde{p},\tilde{m})\}$ is stable for $\beta_1 < \beta < \beta_2$;*

(ii) *at $\beta = \beta_2$, the two-cycle $\{(\tilde{p},\tilde{m}),(-\tilde{p},\tilde{m})\}$ undergoes a 1:2 strong resonance Hopf-bifurcation; for $\beta = \beta_2$ the Jacobian matrix $JF^2((\tilde{p},\tilde{m}))$ has a double eigenvalue $\lambda = -1$, whereas for $\beta \neq \beta_2$, but β close to β_2, the eigenvalues are complex;*

[15] We thank a referee for providing computer simulations showing the creation of two saddle four-cycles in addition to the two stable four-cycles in the secondary bifurcation and for suggesting that this is a strong resonance Hopf bifurcation. This numerical evidence triggered us to prove Theorem 3.4 and show that the secondary bifurcation is a 1:2 strong resonance Hopf bifurcation.

(iii) *for* $\beta > \beta_2$, β *close to* β_2, *the two-cycle* $\{(\tilde{p}, \tilde{m}), (-\tilde{p}, \tilde{m})\}$ *is unstable and four four-cycles exist: a symmetric (with respect to the m-axis) pair of stable four-cycles and a symmetric pair of saddle four-cycles.*

An important feature of the secondary bifurcation is the creation of two coexisting stable four-cycles, which are symmetric with respect to the vertical m-axis. It depends upon the initial state (p_0, m_0) to which of the two stable four-cycles the equilibrium time path will settle down. The *basin of attraction* of an attractor $\mathscr{A}$ is the set of all initial states (p_0, m_0) converging to $\mathscr{A}$. The boundary between two different basins of attraction is called the *basin boundary*. More precisely, a point x lies in the basin boundary if any ε-ball around x contains points from different basins of attraction. It is well known that, in nonlinear systems, the basin boundary can be a very complicated set with a fractal structure (e.g., McDonald, Grebogi, Ott, and Yorke (1985)).

In Figure 7 the basins of attraction of the two stable four-cycles are shown in black and white, for different β-values. The pictures have been obtained by colouring black (white) each initial state of a grid of $M = 350 \times 350$ (the box resolution) equally spaced points, that has converged to an ε-neighborhood (with $\varepsilon = 0.005 <$ screen resolution) of the first (second) stable four-cycle.[16] For $\beta = 2.72$ the two basins are fairly regular and for most initial states it is not difficult to predict to which of the two stable four-cycles the time path converges. For $\beta = 2.74$, however, the situation has changed dramatically. The basin boundary now seems to be a very complicated set with a fractal structure. For higher values of β (e.g. Figure 7d–e) the situation is even more complicated and for most initial states it will be difficult to predict to which of the two stable four-cycles the time path will converge.

McDonald et al. (1985, pp. 126–131) formalized this "final state" unpredictability by the notion of uncertainty dimension. Let B be the basin boundary and J a closed box containing (part of) the basin boundary. An initial state $x \in J$ is called an *ε-uncertainty point* if the ε-ball around x contains initial states from different basins of attraction. Let $f(\varepsilon, J)$ denote the fraction (with respect to Lebesgue measure) of uncertainty points x in J. If the basin boundary B is a smooth curve, then the fraction $f(\varepsilon, J)$ is proportional to ε, i.e. $f(\varepsilon, J) \sim \varepsilon$. However, when B is a more complicated, fractal basin boundary, there can be much worse scaling laws $f(\varepsilon, J) \sim \varepsilon^{\alpha}$, $0 < \alpha < 1$. The *uncertainty exponent* α is then defined as

$$\alpha = \lim_{\varepsilon \to 0} \frac{\ln(f(\varepsilon, J))}{\ln(\varepsilon)}. \tag{3.16}$$

[16] Of all initial states in the 350×350 grid, 99.6% converged to one of the two stable four-cycles, 0.39% converge to the unstable steady state, and only 0.0015% did not converge within 1000 periods.

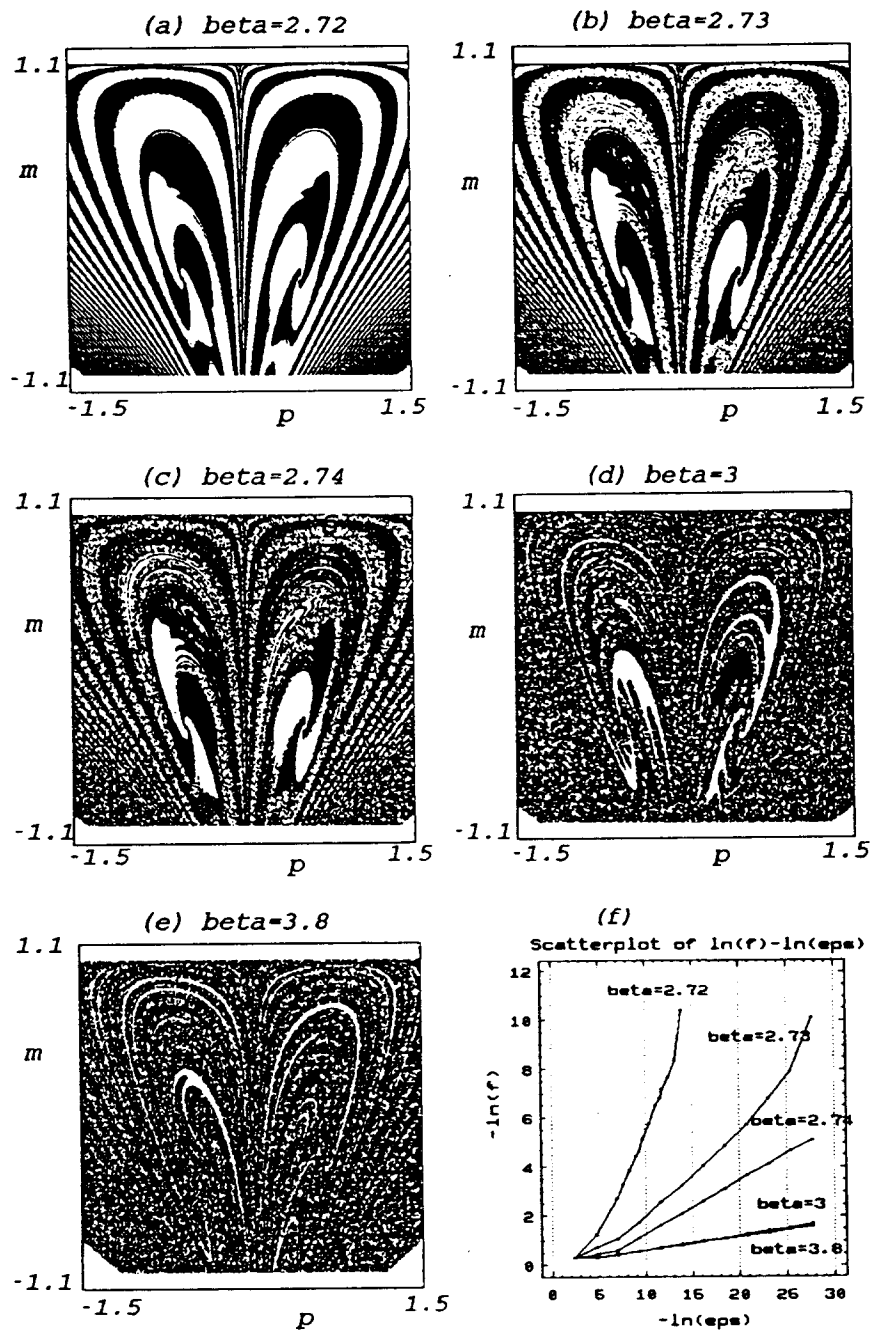

FIGURE 7.—(a)-(e) Basins of attraction of the two coexisting stable 4-cycles for different values of β, with $A = 0$, $B = 0.5$, $b = 1.35$, and $C = 1$; (f) $\ln(f) - \ln(\varepsilon)$ plots, with slope α and uncertainty dimension $D_u = 2 - \alpha$.

TABLE I

ESTIMATES OF THE UNCERTAINTY DIMENSION[a]

β	$\hat{f}$	$\hat{\alpha}$	(SE)	$\hat{D}_u$	$2^{1/\hat{\alpha}}$
2.72	0.190	0.922	(0.007)	1.078	2.1
2.73	0.420	0.366	(0.011)	1.634	6.6
2.74	0.600	0.219	(0.001)	1.781	23.7
3	0.697	0.061	(0.0002)	1.939	86083
3.8	0.723	0.055	(0.0002)	1.945	297353

[a] Estimates of the uncertainty fraction $\hat{f}$, the uncertainty exponent $\hat{\alpha}$, the standard error SE of the linear regression, and the uncertainty dimension $\hat{D}_u$, for β-values corresponding to Figure 7.

The *uncertainty dimension* of B in J is defined as[17]

$$D_u = N - \alpha \tag{3.17}$$

where N is the dimension of the phase space, i.e. $N = 2$ in our case. If the basin boundary is a smooth curve, then $\alpha = 1$ and $D_u = 1$. On the other hand, an uncertainty dimension $D_u > 1$ corresponds to $\alpha < 1$. The uncertainty exponent measures the *sensitive dependence on initial condition uncertainty*. If we want to improve the predictability of the asymptotic final state by a factor 2, we have to increase the accuracy of the initial state by a factor $2^{1/\alpha}$.

Table I summarizes estimates of the uncertainty fraction $\hat{f}$, the uncertainty exponent $\hat{\alpha}$, and the uncertainty dimension $\hat{D}_u$ for β-values corresponding to Figure 7. These estimates have been obtained as follows. Consider the box $J = \{(p, m) \mid -1.5 \le p \le 1.5, -1 \le m \le 1 \text{ and } -m - 1.5 \le p \le m + 1.5\}$ and fix ε. Draw 100,000 random initial states (p_0, m_0) from J. For each of these initial states determine whether (p_0, m_0) and its direct left and right neighbors $(p_0 - \varepsilon, m_0)$ and $(p_0 + \varepsilon, m_0)$ all converge to the same stable four-cycle. If the perturbed initial states do not converge to the same stable four-cycle as the unperturbed initial state, then (p_0, m_0) is an uncertainty point. The estimated uncertainty fraction $\hat{f}(\varepsilon)$ is the number of uncertainty points divided by 100,000. The second column of Table I gives the uncertainty fraction $\hat{f}(\varepsilon)$, where ε is the resolution of the pictures in Figures 7a–e. The same procedure is repeated for each $\varepsilon = 10^{-j}$, $1 \le j \le 12$. The resulting $\ln(f(\varepsilon)) - \ln(\varepsilon)$ plots, for different β-values, are given in Figure 7f. The estimated uncertainty exponent $\hat{\alpha}$ is then

[17] McDonald et al. (1985) and Nusse and Yorke (1992) have shown that, under reasonable assumptions, the uncertainty dimension D_u equals other measures of fractal dimension such as the box counting dimension defined as $D_b = \lim_{\varepsilon \to \infty} \ln(N(\varepsilon, J))/\ln(1/\varepsilon)$, where $N(\varepsilon, J)$ is the minimum number of squares with side ε needed to cover the part of the basin boundary B in J. Strictly speaking these definitions depend on the chosen box J. A natural choice for J is the (bounded) domain of the corresponding map. In numerical experiments like ours, one typically finds the estimates to be independent of J as ε becomes small.

the slope obtained by linear regression[18] and $\hat{D}_u = 2 - \hat{\alpha}$. Our numerical experiments indicate that, as β increases, the uncertainty dimension $\hat{D}_u$ increases and approaches 2. In particular, for $\beta \approx 2.72$ there seems to be an "explosion" of the uncertainty dimension from (close to) 1 up to say 1.6.

These numerical experiments show that, for $2.73 \leq \beta \leq 3.8$, although the long run dynamics is simple, the equilibrium dynamics is sensitive to noise. In the presence of small noise, time paths jump from one basin of attraction to the other in a seemingly random way. As an illustration Figure 8 shows two regular noise free time series converging to each of the two stable four-cycles and one noisy series, with a noisy perfect foresight predictor $H_1(\vec{P}_t) = p_{t+1} + \delta_t$, where δ_t is uniformly distributed over the interval $[-0.02, 0.02]$. The noisy series shows an irregular switching between the two stable four-cycles.

We now will use the DUNRO computer program (Sands and de Vilder (1994)) to show that the complexity and the fractal structure of the basin boundaries for intermediate β-values are caused by a heteroclinic bifurcation.[19] The DUNRO program is a powerful tool for accurate numerical approximation of stable and unstable manifolds of periodic saddles.[20] Using DUNRO we found that, for $\beta \approx 2.728$, the geometric configuration of the stable and unstable manifolds of the two period four-saddles is as indicated in Figure 9b. We have the following theorem.

THEOREM 3.5 (Primary Heteroclinic/Homoclinic Bifurcation): *There exists a $\beta_3 \approx 2.728$ for which a heteroclinic bifurcation between the stable and unstable manifolds of the two saddle four-cycles occurs. For $\beta > \beta_3$ there exist (infinitely) many homoclinic orbits.*

Figure 9 illustrates that the union of the stable manifolds of the symmetric four-saddles $\{z_1, z_2, z_3, z_4\}$ and $\{z_1^*, z_2^*, z_3^*, z_4^*\}$ form the basin boundary between the two symmetric stable four-cycles $\{a_1, a_2, a_3, a_4\}$ and $\{a_1^*, a_2^*, a_3^*, a_4^*\}$. Recall that β_2 is the secondary strong resonance Hopf bifurcation value. Our numerical simulations indicate that for $\beta_2 < \beta < \beta_3$, almost all initial states (except the initial states converging to the unstable steady state, the unstable two-cycle or the four-saddles) converge to one of the two stable four-cycles. For $\beta < \beta_3$, the two branches of the unstable manifold of each of the period 4 saddles approach points of the two *different* stable period 4 orbits. For example, the two branches

[18] For the linear regression, for each β-value the two largest ε-values and the smallest ε-value have been ignored. For ε too large, any point would be an uncertainty point, while for ε too small only few uncertainty points remain out of the 100,000 random initial states.

[19] A *heteroclinic* bifurcation occurs when the stable and unstable manifolds of two *different* periodic saddles are tangent and become transversally intersecting as the parameter varies. We thank one of the referees for providing computer simulations suggesting that a heteroclinic bifurcation might explain the complexity of the basin boundaries.

[20] The method to compute the stable and unstable manifolds, that is implemented in DUNRO, is explained in Homburg, Sands, and de Vilder (1996): see also de Vilder (1995, pp. 145–149) for a description of the program.

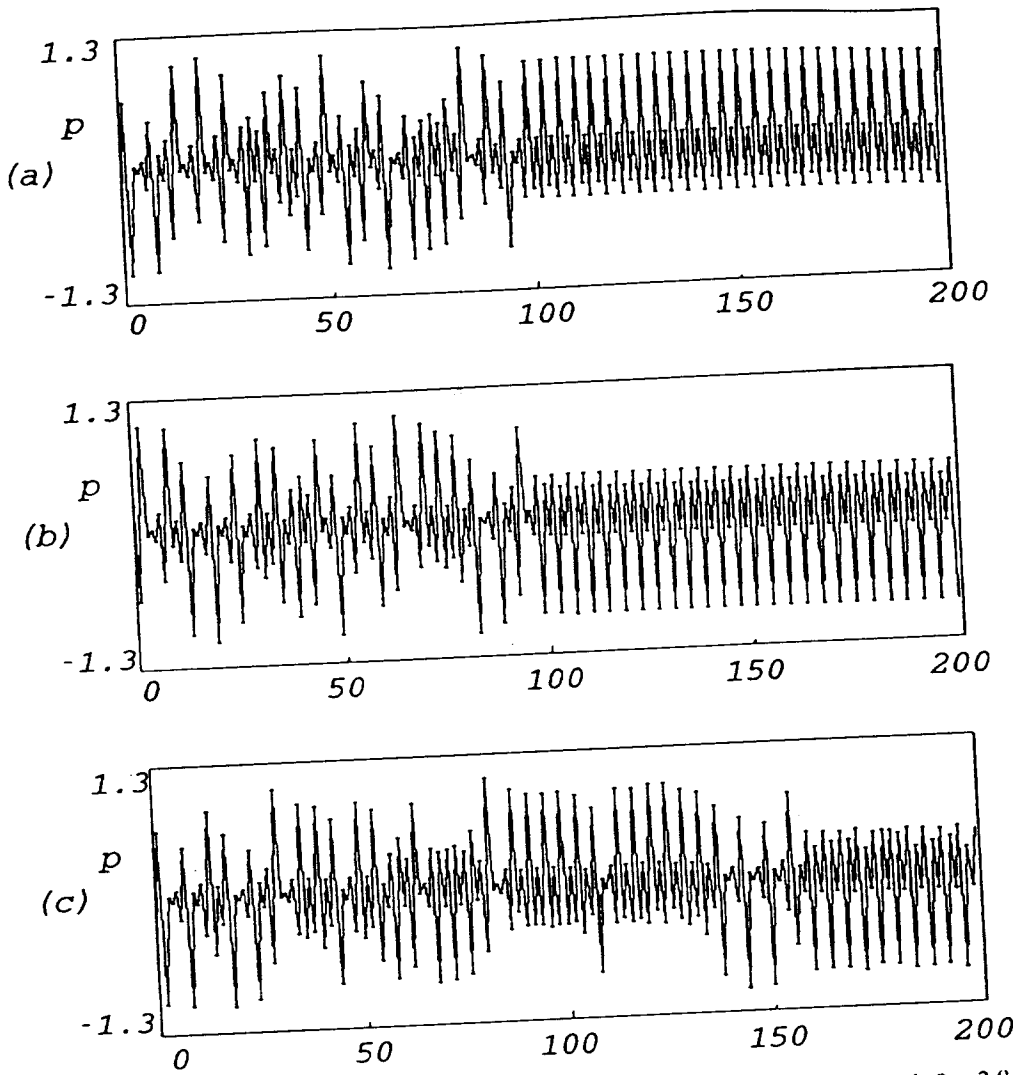

FIGURE 8.—Two coexisting stable 4-cycles for $A = 0$, $B = 0.5$, $b = 1.35$, $C = 1$, and $\beta = 3.8$. (a)-(b) Without noise a typical price time path converges to one of the two stable 4 cycles; (a) $(p_0, m_0) = (0.1, -1)$ and (b) $(p_0, m_0) = (-0.1, -1)$. In the presence of small noise added to the rational expectation predictor, in (c) prices jump erratically between the two basins of attraction of the two four-cycles.

of the unstable manifold of the saddle z_1 approach the stable period 4 points a_1 and a_4^* respectively (Figure 9a). For $\beta < \beta_3$, we did not numerically detect any homoclinic orbits and complicated dynamics, so that β_3 seems to be the critical value at the onset of chaos.[21] At the heteroclinic bifurcation value β_3, one branch of the unstable manifold of z_1 (respectively z_4^*, z_3, and z_2^*) is tangent to the stable manifold of z_4^* (respectively z_3, z_2^*, and z_1). For β only slightly larger

[21] It seems that for $\beta = \beta_3$, our model exhibits a so-called heteroclinic Ω-explosion (see Palis and Takens (1993, Appendix 5)). Our numerical simulations suggest that for $\beta < \beta_3$ the nonwandering set Ω consists of the unstable steady state, the unstable two-cycle and the two stable and two saddle four-cycles. For $\beta > \beta_3$ the nonwandering set Ω has "exploded" into a much more complicated fractal set, including horseshoes.

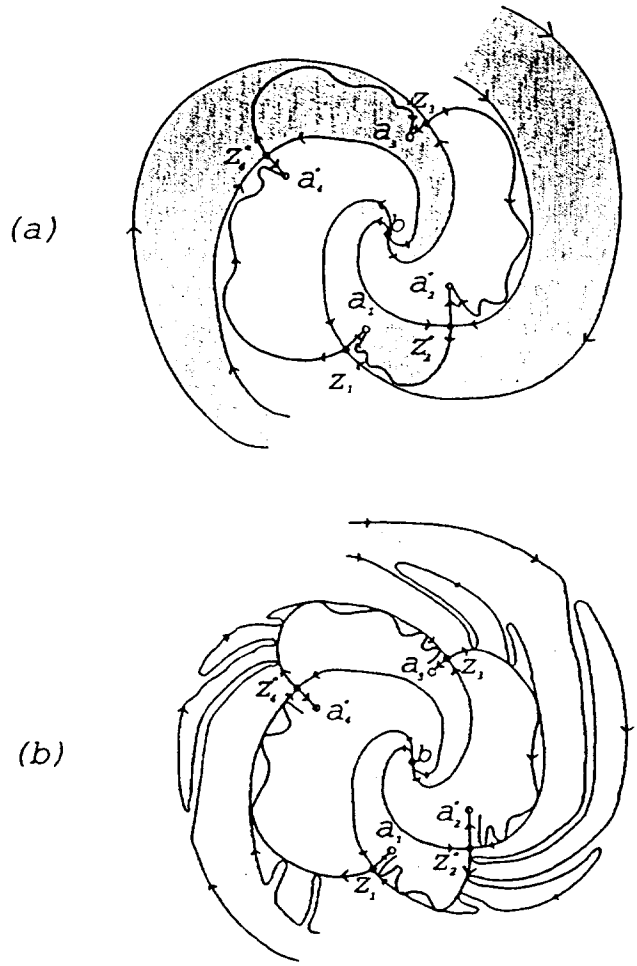

FIGURE 9.—The heteroclinic bifurcation between the two different (symmetric) period four-saddles $\{z_1, z_2, z_3, z_4\}$ and $\{z_1^*, z_2^*, z_3^*, z_4^*\}$. The situation just before the heteroclinic bifurcation is shown in (a), whereas (b) shows the situation at the bifurcation value $\beta = \beta_3 \approx 2.728$. The basins between the two stable four-cycles $\{a_1, a_2, a_3, a_4\}$ and $\{a_1^*, a_2^*, a_3^*, a_4^*\}$ are given by the dark and white regions respectively. The union of the stable manifolds of the four-saddles form the basin boundary. The point b in the center is one of the points of the repelling two-cycle. Only the situation for $p > 0$ is shown; for $p < 0$ the situation is the symmetric opposite.

than β_3, there must be transversal heteroclinic as well as transversal homoclinic intersections. For example, using Figure 9b, the reader may check that for $\beta > \beta_3$ one has:

(i) the left branch of the unstable manifold of z_1 crosses the stable manifold of z_4^*, entering the (dark) basin of attraction of a_3;

(ii) the unstable manifold of z_1 next crosses the stable manifold of z_3, thus entering the (white) basin of attraction of a_2^*;

(iii) the unstable manifold of z_1 next crosses the stable manifold of z_2^*, and enters the (dark) basin of attraction of a_1; and

(iv) the unstable manifold of z_1 next crosses the stable manifold of z_1, and enters the (white) basin of attraction of a_4^*. Hence, there must be homoclinic points associated to the four-saddle $\{z_1, z_2, z_3, z_4\}$.

In particular, it follows that for β slightly larger than β_3, the two basins of attractions of the four-cycles (i.e. the dark and white regions) start "invading each other." The heteroclinic bifurcation in Theorem 3.5 thus explains the fractal structure of the basin boundaries in Figure 7 and the "explosion" of the basin boundary fractal dimension.

The *rational route to randomness* in the cobweb model with rational versus naive expectations may be summarized as follows:

(i) primary period doubling bifurcation for $\beta = \beta_1$ leading to a stable two-cycle;

(ii) secondary 1:2 strong resonance Hopf bifurcation for $\beta = \beta_2$ in which two coexisting stable four-cycles and two four-saddles are created;

(iii) a heteroclinic bifurcation associated to the two four-saddles, for $\beta = \beta_3$, leading to fractal basin boundaries between the two stable four-cycles; immediately after this heteroclinic bifurcation, for intermediate β-values there are also homoclinic bifurcations, leading to strange attractors exhibiting irregular switching between the two saddle four-cycles;

(iv) homoclinic bifurcations associated to period $2N$ saddles, for high values of β, leading to strange attractors characterized by an irregular switching between close to the steady state destabilizing "free riding" and far from the steady state costly, stabilizing sophisticated prediction.

4. FINAL REMARKS

This paper represents an initial foray into developing a theory of evolving selection of prediction strategies. We have introduced the notion of *Adaptive Rational Equilibrium Dynamics* in which the market equilibrium dynamics is coupled to the choice of prediction or learning strategies. We have focussed on a simple analytically tractable example of an A.R.E.D., namely the cobweb model with rational versus naive expectations. This section briefly discusses some future lines of research.

First, we wish to say a few words about the role of limited memory in generating the results of this paper. Our performance or fitness measure for each predictor is net realized profits in the most recent period. It would be interesting to investigate the performance measure with a weighted sum of net realized profits. When all weights are equal (infinite memory), we expect that rational expectations will drive out all other expectational types as time tends to infinity. Formal arguments of this type for related financial models are given in Brock and Hommes (1996c). However, once memory is not infinite and/or if rational expectations are costly to obtain, we expect that complicated dynamics can arise as in the current paper.

In order to investigate the nonlinearity due to predictor selection, we have concentrated on *linear* demand and supply curves. De Fontnouvelle (1995)

presents a financial market model with informed and uninformed traders, and translates it into our cobweb framework with heterogeneous beliefs and nonlinear demand and supply. De Fontnouvelle provides numerical evidence for the period doubling route to chaos. Goeree and Hommes (1997) investigate the cobweb model for nonlinear, monotonic demand and supply curves and find bifurcation routes to strange attractors similar to our linear case.

Our framework can be applied to build other equilibrium models with heterogeneous beliefs. Brock and Hommes (1996a, 1996b) investigate adaptive beliefs in the present discounted value asset pricing model and find complicated dynamics for a large intensity of choice as well, with an irregular switching between close to fundamental fluctuations and upward or downward price trends. In both the cobweb model and the asset pricing model, the market equilibrium equation is linear and one-dimensional. It would be interesting to build A.R.E.D. into other (non)linear market equilibrium models, where agents can choose between two or more predictors. One might try to classify all primary bifurcations of the steady state and the subsequent bifurcation routes to chaos.

A.R.E.D. incorporates a general mechanism for potential local instability of the steady state and complicated global equilibrium dynamics. The two key features generating instability are as follows:

(i) When all agents use the cheapest, "habitual rule of thumb" predictor, the equilibrium steady state is unstable. The endogenous variable starts fluctuating and prediction errors from the cheapest predictor increase.

(ii) When all agents use the costly, sophisticated predictor (e.g. rational expectations, fundamentalists' beliefs, or least squares learning), the endogenous variable converges to its (unique) steady state equilibrium.

In A.R.E.D. satisfying (i) and (ii), for high values of the intensity of choice we expect similar dynamics. The conflict between cheap "free riding" and costly sophisticated prediction is a potential source of instability, homoclinic orbits and chaos. We conjecture that in other equilibrium models with heterogeneous beliefs similar *rational routes to randomness* occur.

Dept. of Economics, University of Wisconsin, 1180 Observatory Dr., Madison, WI 53706, U.S.A.

and

Dept. of Economics, University of Amsterdam, Roetersstraat 11, NL-1018 WB Amsterdam, The Netherlands.

Manuscript received February, 1995; final revision received October, 1996.

APPENDIX

PROOF OF THEOREM 2.1: We show that the linearization of (2.3) at $\vec{P}^*$ is the same as the linearization of (2.7) at $\vec{P}^*$. By Assumption A1, the dynamical system $D(p_{t+1}) = S(H_j(\vec{P}_t))$ has $\vec{P}^*$ as steady state, so $p^* = H_j(\vec{P}^*)$, $j = 1, 2, \ldots, K$. Hence, at the steady state $\vec{P}^*$, $n_{j,t}(p_t, \mathscr{H}(\vec{P}_{t-1})) =$

$n(p^*, \vec{P}^*)$. But

$$\text{(A.1)} \qquad \sum_{j=1}^{K} n(p_t, \mathscr{H}(\vec{P}_{t-1})) = 1, \qquad \text{for all } p_t, \vec{P}_{t-1}$$

implies $n^* \equiv n(p^*, \vec{P}^*) = 1/K$. Next, linearize (2.3) around $\vec{P}^*$ to obtain, letting $\delta p \equiv p - p^*$ and ∇H denote the gradient of H,

$$\text{(A.2)} \qquad D'(p^*)\delta p_{t+1} = \sum_{j=1}^{K} \frac{1}{K} S'(p^*)\nabla H_j(\vec{P}^*)\delta \vec{P}_t + S(p^*) \sum_{j=1}^{K} \delta n(p_t, \mathscr{H}(\vec{P}_{t-1})).$$

But (A.1) implies $\sum \delta n(p_t, \mathscr{H}(P_{t-1})) = 0$, so the second term on the right-hand side of (A.2) drops. Hence, the linearizations of (2.3) and (2.7) are the same. Assumption A2 thus implies that the steady state of (2.3) is locally unstable.

Q.E.D.

PROOF OF THEOREM 2.2: The A.R.E.D. is an $L+1$th order difference equation

$$\text{(2.3)} \qquad D(p_{t+1}) = \sum_{j=1}^{K} n_{j,t}(p_t, \mathscr{H}(\vec{P}_{t-1}))S\left(H_j(\vec{P}_t)\right) = F(p_t, p_{t-1}, \ldots, p_{t-L}),$$

where L is the (maximum) number of lags of the predictors H_j. Let p^* be the steady state price. For any p, $F(p^*, \ldots, p^*, p) = p^*$, since $S(H_j(\vec{P}^*)) = S(p^*)$ and $\sum_{j=1}^{K} n_{j,t} = 1$ for all t. Hence, the partial derivative $F'_{L+1}(p^*, \ldots, p^*, p) = 0$. Using (2.4)–(2.6) we find that the steady state fractions are

$$\text{(A.3)} \qquad n_j^*(\beta) = n_{j,t}(p^*, \mathscr{H}(\vec{P}^*)) = \exp[-\beta C_j]/Z, \qquad Z \equiv \sum_{j=1}^{K} \exp[-\beta C_j].$$

Consider the dynamical system

$$\text{(2.7')} \qquad D(p_{t+1}) = \sum_{j=1}^{K} n_j^*(\beta)S\left(H_j(\vec{P}_t)\right) = G(p_t, p_{t-1}, \ldots, p_{t-L+1}),$$

describing the equilibrium dynamics when the fractions of agents using predictor H_j are fixed at the steady state values of the A.R.E.D. (2.3). The system (2.7′) is an L-dimensional system. Using $F'_{L+1}(p^*, \ldots, p^*, p) = 0$, it can be shown that the eigenvalues of the Jacobian matrix of the steady state of the $L+1$-dimensional system (2.3) are $\lambda = 0$ and the same L eigenvalues corresponding to the Jacobian at the steady state of (2.7′).

For β large, the steady state fraction using the cheapest predictor approaches 1, i.e. $n_K^*(\beta) \approx 1$, whereas $n_j^*(\beta) \approx 0$ for all $j \neq K$. Consider the dynamical system

$$\text{(A.4)} \qquad D(p_{t+1}) = S(H_K(P_t)) = H(p_t, p_{t-1}, \ldots, p_{t-L+1}),$$

describing the equilibrium dynamics when all agents use predictor H_K. By Assumption A2′, the equilibrium steady state $(p^*, \ldots, p^*)$ of (A.4) is locally unstable. Since for β large, the system (2.7′) gets C^1-close to (A.4) we conclude that for β sufficiently large, at the steady state $(p^*, \ldots, p^*)$ the system (2.7′) is locally unstable, implying that the A.R.E.D. (2.3) is also locally unstable at the steady state.

Q.E.D.

PROOF OF THEOREM 3.1: The steady state $(0, \overline{m}(\beta)) = (0, \text{Tanh}(-\beta C/2))$. The eigenvalues of the Jacobian matrix $JF(0, \overline{m})$ at the steady state are 0 and $\lambda(\overline{m}) = -b(1-\overline{m})/[2B + b(1+\overline{m})]$. For $C = 0$, $\overline{m}(\beta) = 0$ and $-1 < \lambda(0) = -b/(2B+b) < 0$, so the steady state is locally stable. Global stability is proven as in (ii) below.

For $C > 0$, as β increases from 0 to $+\infty$, $\overline{m}(\beta)$ decreases from 0 to -1, so $\lambda(\overline{m})$ decreases from $-b/(2B+b)$ to $-b/B < -1$. Hence the steady state becomes an unstable saddle point for some

critical value β_1. For $\beta = \beta_1$, $\lambda(\overline{m}) = -1$ and $\overline{m}(\beta_1) = -B/b$. To prove global stability of the steady state for $\beta < \beta_1$, first note that for all $-1 \le m_t \le 1$, $m_{t+1} \ge \mathrm{Tanh}(-\beta C/2) = \overline{m}(\beta)$, so we may restrict the analysis to initial states with $m_0 \ge \overline{m}$. Define $\lambda(m) = b(1-m)/[2B + b(1+m)]$, so that $p_{t+1} = -\lambda(m_t)p_t$. As m increases from $\overline{m}(\beta)$ to 1, $\lambda(m)$ decreases from $|\lambda(\overline{m})|$ to 0. Hence $|p_{t+1}| \le |\lambda(\overline{m}(\beta))|^t p_0$. Since for all $\beta < \beta_1$, $|\lambda(\overline{m}(\beta))| < 1$ we conclude $p_t \to 0$ and therefore $m_t \to \overline{m}(\beta)$. This proves (ii).

As β increases beyond β_1 a period 2 orbit is created. The symmetry with respect to the m-axis implies that the 2-cycle must be of the form $\{(p_1, \tilde{m}), (p_2, \tilde{m})\}$, where

$$p_2 = \frac{-b(1-\tilde{m})}{2B + b(1+\tilde{m})} p_1. \tag{A.5}$$

Since the same equality must hold with p_1 and p_2 interchanged, we get

$$\frac{-b(1-\tilde{m})}{2B + b(1+\tilde{m})} = -1, \tag{A.6}$$

implying $\tilde{m} = -B/b$. Writing $\tilde{p} = p_1 = -p_2 > 0$ and using (3.9) we find that $\tilde{p}$ satisfies $\mathrm{Tanh}[(\beta/2)(2b\tilde{p}^2 - C)] = -B/b$. This equation has a positive solution $\tilde{p}$ if and only if the steady state value $\overline{m}(\beta) = \mathrm{Tanh}(-\beta C/2) < -B/b$, implying that the two-cycle is indeed created when the steady state becomes unstable at the critical value β_1. Local uniqueness and stability of the two-cycle can be proven by using a standard center manifold reduction (e.g. Guckenheimer and Holmes (1983) or Kuznetsov (1995)). Straightforward computations yield that the one-dimensional map on the center manifold for $\beta = \beta_1$ is given by

$$x_{t+1} = j(x_t) = -x_t + \frac{2b}{B+b}\beta_1 b\left[1 - \left(\frac{B}{b}\right)^2\right] x_t^3 + 0(4). \tag{A.7}$$

Since the third order coefficient is nonzero, the two-cycle is locally unique. According to the period doubling bifurcation theorem (e.g. Guckenheimer and Holmes (1983, p. 158)), the two-cycle is stable, because the coefficient

$$a = \frac{1}{2}j''(0) + \frac{1}{3}j'''(0) = \frac{4b}{B+b}\beta_1 b\left[1 - \left(\frac{B}{b}\right)^2\right] > 0. \qquad Q.E.D.$$

PROOF OF THEOREM 3.2: Obviously, for $\beta = +\infty$, the unique steady state is $E = (0, -1)$. As long as $|p_{t+1} - p_t| \le \sqrt{(2C/b)}$ all firms have naive expectations, but when $|p_{t+1} - p_t| > \sqrt{(2C/b)}$ all firms switch to rational expectations.

For any initial state X, after one time step either all firms have naive expectations or all firms have rational expectations, so we need only consider initial states with $m = -1$ or $m = +1$. For initial states with $m = -1$, not equal to the equilibrium E, since $b/B > 1$ after a number of periods, the price difference will always grow beyond $\sqrt{(2C/b)}$, and then in the next period $m = +1$. An initial state with $m = +1$, will be mapped onto $E = (0, -1)$ or $G = (0, +1)$. Since $F(G) = E$, it follows that all initial states are mapped onto the steady state E, in finite time. *Q.E.D.*

PROOF OF LEMMA 1: Figure 6 illustrates all points defined below and will be helpful in understanding the details of the proof. First take $\beta = +\infty$. Write $C' = (B/(B+b))\sqrt{(2C/b)}$ and define $A_0 = (C', -1)$; A_0 is exactly the point where all agents switch from being naive to becoming rational. We have $A_1 = F_\infty(A_0) = (-(b/B)C', -1)$, $F_\infty(EA_0) = EA_1$, and $A_2 = F_\infty(A_1) = ((b/B)^2 C', +1)$. For each point X denote its reflection point about the m-axis by X^*. We have $F_\infty(EA_0^*) = EA_1^*$. Define $B_0 = (bC'/B, +1)$. It holds that $F_\infty^2(EA_0) = F_\infty(EA_1) = EA_1^* \cup B_0 A_2$ and $F_\infty^2(EA_0^*) = F_\infty(EA_1^*) = EA_1 \cup B_0^* A_2^*$. Let $C_0 = ((b/B)C', 1 - 2B/b)$; then $C_1^- = F_\infty(C_0) = (-C', -1) = A_0^*$ and by symmetry $F_\infty(C_0^*) = C_1^{-*} = A_0$. Let $C_1^+ = (-C', +1)$; then $F_\infty(A_1^* C_0) =$

$A_2^* C_1^+$, $F_\infty(C_0 B_0) = A_0^* E$, and by symmetry $F_\infty(A_1 C_0^*) = A_2 C_1^{+*}$ and $F_\infty(C_0^* B_0^*) = A_0 E$. Two cases have to be distinguished:

CASE 1: $1 < b/B \leq (1+\sqrt{5})/2$ (Figure 6a). In this case $A_3 = F_\infty(A_2) = E$. We have $F_\infty(A_2 C_1^{+*}) = F_\infty(A_2^* C_1^+) = E$, $F_\infty(C_1^{+*} A_0) = EA_1$, and $F_\infty(C_1^+ A_0^*) = EA_1^*$. After including all segments joining points where discontinuous jumps occur, we get $F_\infty^4(EA_0) = EA_1^* B_0 A_2 C_1^{+*} A_0 EA_1^* E$ and by symmetry $F_\infty^4(EA_0^*) = EA_1 B_0^* A_2^* C_1^+ A_0^* EA_1 E$.

CASE 2: $b/B > (1+\sqrt{5})/2$ (Figure 6b). In this case $A_3 = F_\infty(A_2) = G = (0, +1)$ and $F_\infty(B_0) = E$. As in Case 1, $F_\infty(C_1^{+*} A_0) = EA_1$ and $F_\infty(C_1^+ A_0^*) = EA_1^*$. In Case 2, after including all segments joining points where discontinuous jumps occur, we get $F_\infty^4(EA_0) = EA_1^* B_0 A_2 C_1^{+*} A_0 EGEA_1^* E$ and by symmetry $F_\infty^4(EA_0^*) = EA_1 B_0^* A_2^* C_1^+ A_0^* EGEA_1 E$.

By a simple continuity argument (see Brock and Hommes (1995) for details) for β large, the global geometric shape of the unstable manifold now follows: for $\beta < +\infty$, β sufficiently large, the unstable manifold $W_\beta^u(E)$ for F_β is ε-close to $F_\infty^4(EA_0)$ and $F_\infty^4(EA_0^*)$, including all vertical segments where discontinuous jumps occur, as described above. In particular, since the stable manifold $W_\beta^s(E)$ contains the vertical segment EG, there must be an "almost" homoclinic point X close to the point A_0. *Q.E.D.*

PROOF OF LEMMA 2: We will construct a rectangular region R such that the image $F_\beta^4(R)$ is mapped over R in the form of a horseshoe. The geometric shape of the unstable manifold $W_\beta^u(E)$ of the steady state, as described in the proof of Lemma 1, plays a key role in this construction. Brock and Hommes (1995) contains the technical details of the construction; here we concentrate on the main geometric arguments. Let $p_{\max} = p(A_0) = C' = (B/(B+b))\sqrt{(2C/b)}$, $p_{\min} = (B/b)^4 p_{\max}$ and let $0 < \varepsilon \ll p_{\min}$. Define the rectangular region $R = \{(p, m) \mid p_{\min} \leq p \leq p_{\max}, 0 \leq m \leq \varepsilon\}$. Take β sufficiently large so that $W_\beta^u(E)$ is ε-close to $F_\infty^4(EA_0)$ as in the proof of Lemma 1. The unstable manifold $W_\beta^u(E)$ intersects R in the left and right-hand sides of R, as in Figure 6.

F_β is an orientation reversing diffeomorphism and the second iterate F_β^2 an orientation preserving diffeomorphism, on the set $D = \{(p, m) \mid p \in \mathbb{R} \setminus \{0\}, -1 \leq m < 1\}$. For ε small and β large, F_β diffeomorphically maps the region R onto a region $F_\beta(R)$ ε-close to the line segment EA_1, F_β^2 maps the region R diffeomorphically onto the region $F_\beta^2(R)$ ε-close to the piecewise linear segment $EA_1^* B_0 A_2$ and F_β^4 maps the region R diffeomorphically onto the region $F_\beta^4(R)$ ε-close to $F_\infty^4(EA_0)$ (including the vertical segments). Since $p_{\min} = (B/b)^4 p_{\max} = (B/b)^4 p(A_0)$ and $p_{\max} = p(A_0)$, $F_\beta^4(R)$ is a narrow and long stretched region close to $A_0 A_1^* B_0 A_2 C_1^{+*} A_0 E(GE) A_1$ (where GE is excluded when $b/B < (1+\sqrt{5})/2$ (Figure 6a), but included when $b/B > (1+\sqrt{5})/2$ (Figure 6b)). In particular, the rectangular region R contains a smaller rectangle $X_0 Y_0 Z_0 W_0$, with vertices on the upper and lower sides of R and a vertical segment $P_0 Q_0$ such that $F_\beta^4(X_0 Y_0 Z_0 W_0) = X_1 Y_1 Z_1 W_1$ is a horseshoe folded over R, as indicated in Figure 10, with $X_1 Y_1 = F_\beta^4(X_0 Y_0)$ to the right, $P_1 Q_1 = F_\beta^4(P_0 Q_0)$ to the left and $Z_1 W_1 = F_\beta^4(Z_0 W_0)$ to the right of R. We conclude that F_β^4 has a full horseshoe. *Q.E.D.*

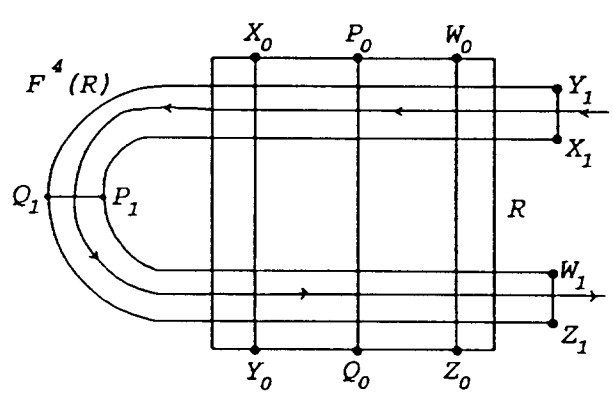

FIGURE 10.—$F_\beta^4(R)$ is mapped over the rectangular region R in the form of a horseshoe.

PROOF OF LEMMA 3: Define the rectangular region $R_N = \{(p,m) \mid ((b/B)^{2N-4}p, m) \in R\}$, with the rectangular region R defined as in the proof of Lemma 2. Using the global shape of the unstable manifold of the steady state $W^u_\beta(E)$, a similar construction as in the proof of Lemma 2 shows that R_N contains a smaller rectangular region Q, such that the images $F^{2N-2}(Q)$ and $F^{2N}(Q)$ have the form of horseshoes close to $W^u_\beta(E)$, as in Figure 6c–d. We have indicated points $D_{j+1} = F^2(D_j)$, $j = 0, 1$, of $W^u_\beta(E)$ close to the p-axis. For β large, the distance between D_{j+1} and the m-axis is approximately $(b/B)^2$ times the distance between D_j and the m-axis, $j = 0$ or 1. As β increases the points D_j, $0 \le j \le 2$, move closer to the m-axis and therefore $F^{2N}(Q)$ also moves to the m-axis and a horseshoe for F^{2N} is created as in Figure 6d. The creation of these horseshoes implies the occurrence of homoclinic bifurcations (see Palis and Takens (1993, p. 14–16)). It remains to be shown that, for N large, the period $2N$ saddle points are dissipative, i.e. the product of the eigenvalues of JF^{2N} is smaller than 1 in modulus. The region R_N moves closer to the stable manifold (the m-axis) as N increases, so for large N, most points of the period $2N$ saddle are close to the steady state. The fact that the steady state is a dissipative saddle point (an eigenvalue $\lambda = 0$) implies that, for N sufficiently large, the period $2N$ saddle is also dissipative (Palis and Takens (1993, p. 29, Remark 2)). *Q.E.D.*

PROOF OF THEOREM 3.3: This follows immediately from the homoclinic bifurcations associated to dissipative period $2N$-saddles in Lemma 3 and the "strange attractor theorem," in subsection 3.3. For generic demand and supply curves C^2-close to the linear curves, the geometric construction in the proof of Lemma 3 is the same and the generic conditions concerning the homoclinic bifurcations will be satisfied, so the "strange attractor theorem" applies. *Q.E.D.*

PROOF OF THEOREM 3.4: Write $F(p,m) = (f(p,m), g(p,m))$. The two-cycle is $\{(\bar{p}, \bar{m}), (-\bar{p}, \bar{m})\}$, with $\bar{m} = -B/b$ and $\bar{p}$ the positive solution of $\mathrm{Tanh}[(\beta/2)(2b\bar{p}^2 - C)] = \bar{m}$, and write $\phi(z)$ for $\mathrm{Tanh}(z)$. Using $f(\bar{p}, \bar{m}) = -\bar{p}$ and $f'_p(\pm\bar{p}, \bar{m}) = -1$, a straightforward computation yields the Jacobian matrix at the period 2 point $(\bar{p}, \bar{m})$:

$$\text{(A.8)} \qquad JF(\bar{p}, \bar{m}) = \begin{pmatrix} -1 & \dfrac{2b\bar{p}}{b+B} \\ 2b\beta\bar{p}\phi'\left(\dfrac{\beta}{2}(2b\bar{p}^2 - C)\right) & -2b\beta\dfrac{b}{b+B}\bar{p}^2\phi'\left(\dfrac{\beta}{2}(2b\bar{p}^2 - C)\right) \end{pmatrix}$$

or writing $\gamma = b\bar{p}/(b+B)$ and $\delta = 2b\beta\bar{p}\phi'((\beta/2)(2b\bar{p}^2 - C))$,

$$\text{(A.9)} \qquad JF(\bar{p}, \bar{m}) = \begin{pmatrix} -1 & 2\gamma \\ \delta & -\gamma\delta \end{pmatrix} \quad \text{and} \quad JF(-\bar{p}, \bar{m}) = \begin{pmatrix} -1 & -2\gamma \\ -\delta & -\gamma\delta \end{pmatrix}.$$

Stability of the two-cycle is determined by $JF^2(\bar{p}, \bar{m}) = JF(-\bar{p}, \bar{m})JF(\bar{p}, \bar{m})$, giving

$$\text{(A.10)} \qquad JF^2(\bar{p}, \bar{m}) = \begin{pmatrix} 1 - 2\gamma\delta & 2\gamma^2\delta - 2\gamma \\ \delta - \gamma\delta^2 & -2\gamma\delta + \gamma^2\delta^2 \end{pmatrix}.$$

The characteristic equation for the eigenvalues of $JF^2(\bar{p}, \bar{m})$ is

$$\text{(A.11)} \qquad \lambda^2 - \lambda(\gamma^2\delta^2 - 4\gamma\delta + 1) + \gamma^2\delta^2 = 0,$$

with discriminant $D = (\gamma\delta - 1)^2(\gamma^2\delta^2 - 6\gamma\delta + 1)$. When β increases from 0 to $+\infty$, $\bar{p}$ increases from 0 to $\sqrt{(C/2b)}$ and $\phi'((\beta/2)(2b\bar{p}^2 - C))$ increases from 0 to $+\infty$, so $\gamma = b\bar{p}/(b+B)$ increases from 0 to $(b/(b+B))\sqrt{(C/2b)}$, $\delta = 2b\beta\bar{p}\phi'((\beta/2)(2b\bar{p}^2 - C))$ increases from 0 to $+\infty$ and in particular $\gamma\delta$ increases from 0 to $+\infty$. The reader may easily verify that for $3 - 2\sqrt{2} < \gamma\delta < 3 + 2\sqrt{2}$, the discriminant $D < 0$, except when $\gamma\delta = 1$ where $D = 0$. Moreover, the product of the eigenvalues

is $\gamma^2\delta^2$. Let β_2 and β^* be the values of β for which $\gamma\delta = 1$, respectively $\gamma\delta = 3 + 2\sqrt{2}$. It is then clear that for $\beta < \beta_2$, β close to β_2, the period 2 cycle is stable with complex eigenvalues, for $\beta = \beta_2$ $JF^2(\bar{p}, \bar{m})$ has a double eigenvalue -1, and for $\beta_2 < \beta < \beta^*$ the two-cycle is unstable with complex eigenvalues. For $\beta = \beta_2$ the two-cycle $\{(\bar{p}, \bar{m}), (-\bar{p}, \bar{m})\}$ thus undergoes a strong resonance 1:2 Hopf bifurcation. This proves (i) and (ii).

In order to prove the creation of two stable and two saddle four-cycles in the secondary bifurcation for $\beta = \beta_2$, we have to compute the corresponding normal form. These normal form computations are simplified by exploiting the symmetry with respect to the m-axis, thus reducing the 1:2 strong resonance Hopf bifurcation of a two-cycle of F, to a 1:4 strong resonance Hopf bifurcation[22] of a fixed point of the map $G = FT$, where

$$T = \begin{pmatrix} -1 & 0 \\ 0 & 1 \end{pmatrix}.$$

Brock and Hommes (1995) compute the normal form in complex coordinates to be

$$z_{t+1} = (1 + \mu)e^{i\nu}z_t + Qz_t^2\bar{z}_t + R\bar{z}_t^3 + O(5), \tag{A.12}$$

with (in three decimals accuracy), $Q = q_1 + q_2 i = 0.947 - 1.211i$ and $R = r_1 + r_2 i = 0.024 - 0.285i$ and show that two four-cycles bifurcate from the steady state, one sink and one saddle. It then follows that for $\beta > \beta_2$ and β close to β_2 the map $G = FT$ has a stable four-cycle $\{a_1, a_2, a_3, a_4\}$ and a four-saddle $\{z_1, z_2, z_3, z_4\}$. Using the symmetry $FT = TF$, it then follows that $\{a_1, Ta_2, a_3, Ta_4\}$ and its symmetric opposite $\{Ta_1, a_2, Ta_3, a_4\}$ are two stable four-cycles of the map F and the symmetric pair $\{z_1, Tz_2, z_3, Tz_4\}$ and $\{Tz_1, z_2, Tz_3, z_4\}$ are two four-saddles of F. *Q.E.D.*

PROOF OF THEOREM 3.5: This proof is computer assisted. Using the DUNRO program (Sands and de Vilder (1994)) yields accurate numerical approximations of the stable and unstable manifolds of periodic saddles. For $\beta = \beta_3 \approx 2.72$ we find a heteroclinic bifurcation between the period 4 saddle $\{z_1, z_2, z_3, z_4\}$ and its symmetric opposite $\{z_1^*, z_2^*, z_3^*, z_4^*\}$ as indicated in Figure 9. From this geometric configuration it follows that for $\beta > \beta_3$ there must be (infinitely many) homoclinic orbits associated to each of the two period 4 saddles. *Q.E.D.*

REFERENCES

ANDERSON, S., A. DE PALMA, AND J. THISSE (1993): *Discrete Choice Theory of Product Differentiation*. Cambridge, Mass.: MIT Press.

ARNOLD, V. I. (1988): *Geometrical Methods in the Theory of Ordinary Differential Equations*, 2nd ed. Berlin: Springer Verlag.

ARTHUR, B. (1992): "On Learning and Adaptation in the Economy," Santa Fe Institute Paper 92-07-038.

ARTHUR, B., J. HOLLAND, B. LEBARON, R. PALMER, AND P. TAYLOR (1994): "An Artificial Stock Market," Santa Fe Institute Working Paper, September, 1994.

C. AZARIADIS, AND B. SMITH (1994): "Regime Switching in Business Cycles," Department of Economics, UCLA and Cornell.

BENEDICKS, M., AND L. CARLESON (1991): "The Dynamics of the Hénon Map," *Annals of Mathematics*, 133, 73–169.

BENHABIB, J., AND R. H. DAY (1982): "A Characterization of Erratic Dynamics in the Overlapping Generations Model," *Journal of Economic Dynamics & Control*, 4, 37–55.

[22] The 1:4 strong resonance Hopf bifurcation is one of the most complicated local (codimension 2) bifurcations and it seems that the details of this bifurcation are still not completely understood (see, e.g., Arnold (1988), Whitley (1983), Gambaudo (1985), Lauwerier (1986), and Kuznetsov (1995)). The first revised version of this paper, Brock and Hommes (1995, SSRI Working Paper 9530) contains the detailed normal form computations.

BLUME, L., AND D. EASLEY (1992): "Evolution and Market Behavior," *Journal of Economic Theory*, 58, 9–40.

BROCK, W. (1993): "Pathways to Randomness in the Economy: Emergent Nonlinearity and Chaos in Economics and Finance," *Estudios Economicos*, 8, 3–55.

BROCK, W. A., AND C. H. HOMMES (1995): "Rational Routes to Randomness," SSRI Working Paper 9506 (revised version 9530), Dept. of Economics, Univ. of Wisconsin.

——— (1996a): "Models of Complexity in Economics and Finance," Department of Economics, Univ. of Amsterdam, Report AE 5/96.

——— (1996b): "Heterogeneous Beliefs and Routes to Chaos in a Simple Asset Pricing Model," Tinbergen Institute Discussion Paper, TI 96-147/8, University of Amsterdam.

——— (1996c): "Adaptive Beliefs and the Emergence of Complex Dynamics in Asset Pricing Models," Dept. of Economics, Univ. of Wisconsin.

BROCK, W., AND LEBARON, B. (1996): "A Dynamic Structural Model for Stock Return Volatility and Trading Volume," *Review of Economics and Statistics*, 78, 94–110.

CABRALES, A., AND T. HOSHI (1996): "Heterogeneous Beliefs, Wealth Accumulation, and Asset Price Dynamics," *Journal of Economic Dynamics & Control*, 20, 1073–1100.

CHIARELLA, C. (1992): "The Dynamics of Speculative Behaviour," *Annals of Operations Research*, 37, 101–123.

DE GRAUWE, P., H. DEWACHTER, AND M. EMBRECHTS (1993): *Exchange Rate Theory. Chaotic Models of Foreign Exchange Markets*. Oxford: Blackwell.

EVANS, G., AND S. HONKAPOHJA (1994): "Adaptive Learning and Expectational Stability: An Introduction," in *Learning and Rationality in Economics*, ed. by A. Kirman and M. Salmon. Oxford: Blackwell.

EVANS, G., AND G. RAMEY (1992): "Expectation Calculation and Macroeconomic Dynamics," *American Economic Review*, 82, 207–224.

DE FONTNOUVELLE, P. (1995): "Informational Strategies in Financial Markets: The Implications for Volatility and Trading Volume Dynamics," Department of Economics, Iowa State University.

GAMBAUDO, J. M. (1985): "Perturbation of a Hopf Bifurcation by an External Time-Periodic Forcing," *Journal of Differential Equations*, 57, 172–199.

GOEREE, J., AND HOMMES, C. H. (1997): "Heterogeneous Beliefs in the Nonlinear Cobweb Model," Working Paper, Dept., of Econ., Univ. of Amsterdam.

GRANDMONT, J.-M. (1985): "On Endogenous Competitive Business Cycles," *Econometrica*, 53, 995–1045.

——— (1994): "Expectations Formation and Stability of Large Socioeconomic Systems," CEPREMAP W.P. No. 9424.

GRANDMONT, J.-M., AND G. LAROQUE (1991): "Economic Dynamics with Learning: Some Instability Examples," in *Equilibrium Theory and Applications: Proceedings of the Sixth International Symposium in Economic Theory and Econometrics*, ed. by W. A. Barnett, B. Cornet, C. d'Aspremont, J. Gabscewicz, and A. Mas-Colell. Cambridge: Cambridge University Press, pp. 247–273.

GUCKENHEIMER, J., AND P. HOLMES (1983): *Nonlinear Oscillations, Dynamical Systems, and Bifurcations of Vector Fields*. New York: Springer-Verlag.

GUESNERIE, R., AND M. WOODFORD (1992): "Endogenous Fluctuations," in *Advances in Economic Theory: Sixth World Congress*, ed. by J. J. Laffont. Cambridge: Cambridge University Press.

HOMBURG, A. J., D. J. SANDS, AND R. G. DE VILDER (1996): "Computing Invariant Sets," Working Paper, University of Amsterdam.

HOMMES, C. H. (1991): *Chaotic Dynamics in Economic Models: Some Simple Case Studies*. Groningen, The Netherlands: Wolters-Noordhoff.

——— (1994): "Dynamics of the Cobweb Model with Adaptive Expectations and Nonlinear Supply and Demand," *Journal of Economic Behavior & Organization*, 24, 315–335.

——— (1997): "On the Consistency of Backward Looking Expectations. The Case of the Cobweb," forthcoming in *Journal of Economic Behaviour & Organization*.

KIEFER, N., Z. YE, AND M. AN (1993): "A Dynamic Model of Local and Global Interactions Among Economic Agents," Dept. of Economics, Cornell University.

KURZ, M. (1994): "On Rational Belief Equilibria," *Economic Theory*, 4, 859–876.

KUZNETSOV, Y. A. (1995): *Elements of Applied Bifurcation Theory*. Berlin: Springer-Verlag.

LAUWERIER, H. A. (1986): "Two-dimensional Iterative Maps," in *Chaos*, ed. by A. V. Holden. Manchester: Manchester University Press.

LUX, T. (1995): "Herd Behaviour, Bubbles and Crashes," *The Economic Journal*, 105, 881–896.

MANSKI, C., AND D. MCFADDEN (1981): *Structural Analysis of Discrete Data with Econometric Applications*. Cambridge: MIT Press.

MARCET, A., AND T. SARGENT (1989): "Convergence of Least Squares Learning in Environments with Hidden State Variables and Private Information," *Journal of Political Economy*, 97, 1306–1322.

MARIMON, R. (1993): "Adaptive Learning, Evolutionary Dynamics, and Equilibrium Selection," *European Economic Review*, 37, 603–611.

MCDONALD, S., C. GREBOGI, E. OTT, AND J. YORKE, (1985): "Fractal Basin Boundaries," *Physica*, 17D, 125–153.

MORA, L., AND M. VIANA (1993): "Abundance of Strange Attractors," *Acta Mathematica*, 171, 1–71.

NUSSE, H. E., AND J. A. YORKE (1992): "The Equality of Fractal Dimension and Uncertainty Dimension for Certain Dynamical Systems," *Communications in Mathematical Physics*, 150, 1–21.

PALIS, J., AND F. TAKENS (1993): *Hyperbolicity and Sensitive Chaotic Dynamics at Homoclinic Bifurcations*. Cambridge: Cambridge University Press.

PINTUS, P., D. J. SANDS, AND R. DE VILDER (1996): "On the Transition from Local Regular to Global Irregular Fluctuations," Working Paper, CEPREMAP.

POINCARÉ, H. (1890): "Sur le Problème des Trois Corps et les Equations de la Dynamique" (Mémoire couronné du prise de S. M. le roi Oscar II de Suède), *Acta Mathematica*, 13, 1–270.

SANDS, D. J., AND R. G. DE VILDER (1994): "DUNRO: A Global Bifurcation Analyzer," University of Amsterdam.

SARGENT, T. (1993): *Bounded Rationality in Macroeconomics*. Oxford: Clarendon Press.

SETHI, R. (1996): "Endogenous Regime Switching in Speculative Markets," *Structural Change and Economic Dynamics*, 7, 99–118.

SMALE, S. (1965): "Diffeomorphisms with Many Periodic Points," in *Differential and Combinatorial Topology*, ed. by S. S. Cairns. Princeton, NJ: Princeton Univ. Press, 63–80.

TAKENS, F. (1992): "Abundance of Generic Homoclinic Tangencies in Real-Analytic Families of Diffeomorphisms," *Boletim da Sociedade Brasileira de Matemática*, 22, 191–214.

TOWNSEND, R. (1983): "Forecasting the Forecasts of Others," *Journal of Political Economy*, 91, 546–588.

VILDER, DE R. (1995): "Endogenous Business Cycles," Thesis, Department of Economics, Tinbergen Institute Research Series 96, University of Amsterdam.

——— (1996): "Complicated Endogenous Business Cycles under Gross Substitutability," *Journal of Economic Theory*, 71, 416–442.

WHITLEY, C. (1983): "Discrete Dynamical Systems in Dimensions One and Two," *Bulletin of the London Mathematical Society*, 15, 177–217.